Journal of Alloys and Compounds 480 (2009) 246–253

Contents lists available at ScienceDirect

Journal of Alloys and Compounds

journal homepage: www.elsevier.com/locate/jallcom

Structure, microstructure and electrical properties of $(1-x-y)Bi_{0.5}Na_{0.5}TiO_3$–$xBi_{0.5}K_{0.5}TiO_3$–$yBi_{0.5}Li_{0.5}TiO_3$ lead-free piezoelectric ceramics

Zupei Yang*, Yuting Hou, Hong Pan, Yunfei Chang

Key Laboratory for Macromolecular Science of Shaanxi Province, School of Chemistry and Materials Science, Shaanxi Normal University, Xi'an, 710062 Shaanxi, PR China

ARTICLE INFO

Article history:
Received 22 October 2008
Received in revised form 23 January 2009
Accepted 8 February 2009
Available online 21 February 2009

Keywords:
Ceramics
Microstructure
Dielectric properties
Ferroelectrics
Piezoelectricity

ABSTRACT

The ternary system $(1-x-y)Bi_{0.5}Na_{0.5}TiO_3$–$xBi_{0.5}K_{0.5}TiO_3$–$yBi_{0.5}Li_{0.5}TiO_3$ (abbreviated to BNKLT-x/y) was synthesized by conventional oxide-mixed method. The phase structure, microstructure, and dielectric, ferroelectric and piezoelectric properties of the ceramics were investigated. The X-ray diffraction patterns showed that pure perovskite phase with rhombohedral structure can be obtained in all the ceramics. The grain size varied with x and y. The temperature dependence of dielectric constant and dielectric loss revealed there were two phase transitions which were from ferroelectric (tetragonal) to anti-ferroelectric (rhombohedral) and anti-ferroelectric to paraelectric (cubic). Either increasing x or y content can make T_m (the temperature at which dielectric constant ε_r reaches the maximum) increase. With the addition of $Bi_{0.5}K_{0.5}TiO_3$, the remanent polarization P_r increased but the coercive field E_c decreased. With the addition of $Bi_{0.5}Li_{0.5}TiO_3$, P_r increased obviously and E_c increased slightly. Due to the stronger ferroelectricity by modifying $Bi_{0.5}K_{0.5}TiO_3$ and $Bi_{0.5}Li_{0.5}TiO_3$, the piezoelectric properties were enhanced at $x = 0.22$ and $y = 0.10$, which were as follows: $P_r = 31.92\ \mu C/cm^2$, $E_c = 32.40$ kV/cm, $\varepsilon_r = 1118$, $\tan\delta = 0.041$, $d_{33} = 203$ pC/N and $K_p = 0.31$. The results show that the BNKLT-x/y ceramics are promising candidates for the lead-free materials.

1. Introduction

It is well known that piezoelectric materials markets are dominated by $Pb(Zr_xTi_{1-x})O_3$ (abbreviated to PZT) based ceramics due to their excellent electrical properties. However, because of the toxicity of PbO and its high vapor pressure during sintering process, using lead-based ceramics causes not only serious environmental problems but also produces unstability of composition. So it is very urgent to develop lead-free piezoelectric ceramics with excellent properties to replace PZT based ceramics.

$Bi_{0.5}Na_{0.5}TiO_3$ (abbreviate to BNT), discovered by Smolenskii et al. [1], is an ABO_3 type ferroelectric with perovskite phase. BNT is considered to be a promising candidate of lead-free piezoelectric ceramics with a relatively large remanent polarization ($P_r = 38\ \mu C/cm^2$) and a high Curie temperature ($T_c = 320\ ^\circ C$) [2–4]. However, the pure BNT ceramics have the drawbacks of high conductivity and high coercive field, which can induce problems in poling process and limit their applications. In order to get BNT-based ceramics with optimum properties, new BNT-based systems have been investigated, such as BNT–$BaTiO_3$ [5], BNT–$Bi_{0.5}K_{0.5}TiO_3$ [6], BNT–$BaTiO_3$–$Ba(Ti,Zr)O_3$ [7], BNT–$BaTiO_3$–$K_{0.5}Na_{0.5}NbO_3$ [8], BNT–$K_{0.5}Na_{0.5}NbO_3$ [9] and so on. According to our previous work [6], introducing $Bi_{0.5}K_{0.5}TiO_3$ (abbreviate to BKT) could enhance the electrical properties of BNT ceramics. Lin et al. [10] found that introduction of $Bi_{0.5}Li_{0.5}TiO_3$ (abbreviate to BLT) could decrease sintering temperature and improve the densification of the BNT–$BaTiO_3$ ceramics.

In this work, y was fixed at 0.10. Then x was changed from 0.16 to 0.26 when $y = 0.10$. The optimum value of x was found. Then x was fixed at its optimum value 0.22, and y was changed from 0.03 to 0.12. The optimum value of y was found. BNT-based lead-free piezoelectric ceramics BNKLT-x/y were synthesized by conventional mixed-oxide method and the effects of $Bi_{0.5}K_{0.5}TiO_3$ and $Bi_{0.5}Li_{0.5}TiO_3$ contents on the structure, microstructure, dielectric, ferroelectric and piezoelectric properties was investigated systematically.

2. Experimental

Conventional mixed-oxide method was adopted to prepare $(1-x-y)Bi_{0.5}Na_{0.5}TiO_3$–$xBi_{0.5}K_{0.5}TiO_3$–$yBi_{0.5}Li_{0.5}TiO_3$ with $x = 16$–22 mol% and $y = 3$–12 mol%. Reagent grade Bi_2O_3 (99%), Na_2CO_3 (99.8%), K_2CO_3 (99%), Li_2CO_3

* Corresponding author. Tel.: +86 29 8531 0352; fax: +86 29 8530 7774.
E-mail address: yangzp@snnu.edu.cn (Z. Yang).

0925-8388/$ – see front matter © 2009 Elsevier B.V. All rights reserved.
doi:10.1016/j.jallcom.2009.02.030

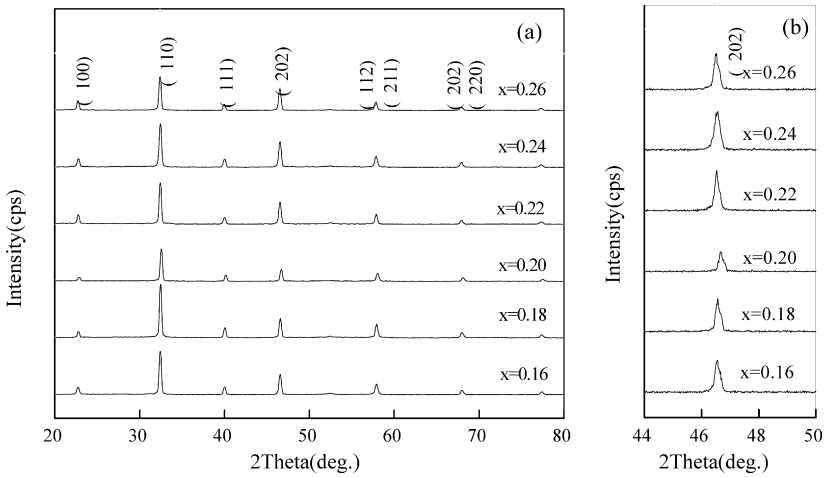

Fig. 1. XRD patterns of BNKLT-x/0.10 ceramics.

(98%) and TiO_2 (99.1%) were used as starting materials. First, these oxides or carbonate powders were weighed in appropriate stoichiometry according to the reaction (1), and mixed in ethanol with zirconium balls by ball-milling for 12 h.

$$(1-x-y)/4Na_2CO_3 + x/4K_2CO_3 + y/4Li_2CO_3 + 0.25Bi_2O_3 + TiO_2 = (1-x-y)Bi_{0.5}Na_{0.5}TiO_3 - x\,Bi_{0.5}K_{0.5}TiO_3 - yBi_{0.5}Li_{0.5}TiO_3 + 0.25CO_2\uparrow \quad (1)$$

After being dried, the powders were calcined at 850 °C for 2 h in air. The calcined powders were detected by X-ray diffraction and all samples exhibited pure perovskite phase. Then the calcined powders were mixed with polyvinyl alcohol and pressed into discs with a diameter of 15 mm under 100 MPa. The green pellets were sintered at 1130 °C in air. The sintered ceramics were detected by X-ray diffraction and all samples exhibited pure perovskite phase. Silver pastes were fired on both sides of the discs as electrodes. The specimens were poled in silicon oil at 80 °C under 3–4 kV/mm for 15 min.

The crystalline phase structure of the ceramics was analyzed by X-ray diffraction (XRD, Model DMX-2550/PC, Rigaku, Japan) using Cu Kα radiation. The microstructure of the sintered ceramics was observed by using scanning electron microscopy (SEM Model Quanta 200, FEI Company). The bulk densities were measured by Archimedes method.

Dielectric properties of the ceramics were obtained by measuring capacitance C and dielectric loss tan δ using a LCR meter (HP 4294A) at room temperature. Temperature dependence of dielectric constant ε_r and dielectric loss tan δ were measured by a LCR meter (Agilent 4294A) from room temperature to 450 °C at 1, 10 and 100 kHz. The piezoelectric constant d_{33} was measured by a quasi-static piezoelectric d_{33} meter (Model ZJ-3d, Institute of Acoustics Academic Sinica, China). The electromechanical coupling factor K_p was calculated from the resonance and anti-resonance frequencies based on the IEEE standards using an impedance analyzer (HP 4294A). The polarization versus electric (P–E) hysteresis loops were observed by a Radiant Precision Workstation (USA) at 100 Hz.

3. Results and discussion

Figs. 1 and 2 show the X-ray diffraction patterns of the BNKLT-x/y ceramics. It can be seen that all the samples present pure perovskite phase and no secondary phase can be detected, which means that K^+ and Li^+ have diffused into the lattice to form a solid solution. The diffraction peaks are indexed according to JCPDS card NO. 36-0340. According to the reports that one peak near 47° indicates all samples have rhombohedral symmetry structure and a splitting peak near 47° indicates the tetragonality of the samples [11–13]. Figs. 1(b) and 2(b) are the magnifications of Figs. 1(a) and 2(a) in the range from 45° to 50° respectively. The feature peak at about 47° does not split in the two figures, which indicates that all ceramics have rhombohedral symmetry structure.

The SEM micrographs of BNKLT-x/0.10 and BNKLT-0.22/y ceramics are exhibited in Figs. 3 and 4. All ceramics show a quasi-cubic morphology with clear grain boundaries. The morphology of the ceramics is similar to result of other investigations [14–16]. In Fig. 3, with increasing x from 0.16 to 0.22, the average grain size decreases from 3.0 to 2.0 μm. Then further increasing x, the change of the grain size is not obvious. It can also be seen that the ceramics with relatively homogenous microstructure and fewer pores can be obtained at x = 0.22. Besides, when y = 0.03, the average grain size is about 1.0 μm. With increasing y, the grain size increases obviously. When y reaches 0.10, the average grain size is 2.0 μm and the ceramics are compact with fewer pores (Fig. 4). Results of Figs. 3 and 4 have

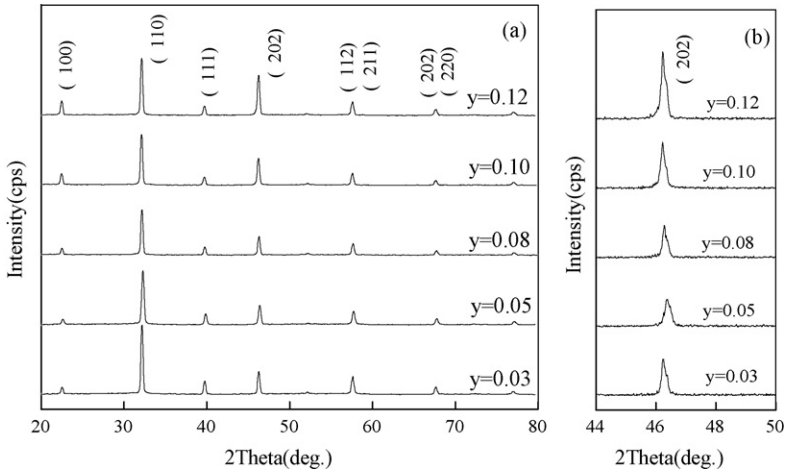

Fig. 2. XRD patterns of BNKLT-0.22/y ceramics.

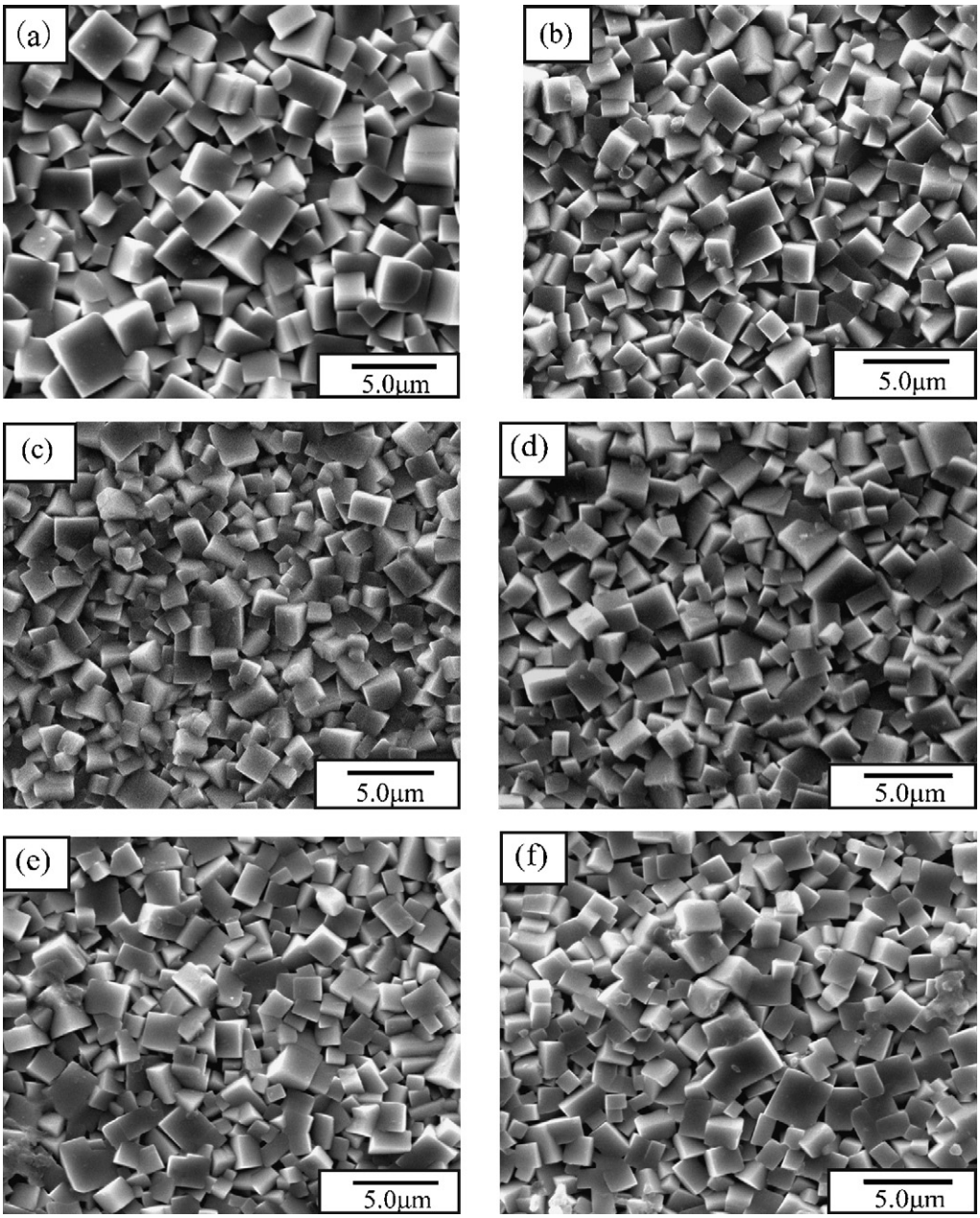

Fig. 3. SEM micrographs of BNKLT-*x*/0.10 ceramics: (a) $x = 0.16$; (b) $x = 0.18$; (c) $x = 0.20$; (d) $x = 0.22$; (e) $x = 0.24$; (f) $x = 0.26$.

shown that the relatively compact and homogenous microstructure can be obtained at $x = 0.22$ and $y = 0.1$.

Fig. 5 shows the density of the BNKLT ceramics with different x and y. It can be seen from Fig. 5(a) that with increasing x from 0.16 to 0.22, the density increases and reaches maximum value of 5.76 g/cm^3 at 0.22. The ceramics have higher density than that of our previous work [6]. Further increasing x to 0.26 causes the decrease of it to 5.45 g/cm^3. It can also be seen from Fig. 5(b) that as y varies from 0.03 to 0.12, the density of the ceramics increases from 5.35 to the maximum value (5.76 g/cm^3) at $y = 0.10$, and then drops to 5.48 g/cm^3 with further increasing y to 0.12. The result of Fig. 5 indicates that the ceramics with $x = 0.22$ and $y = 0.10$ show the maximum value of the density, which is in accordance with those of Figs. 3 and 4.

Figs. 6 and 7 show the temperature dependence of dielectric constant ε_r and dielectric loss tan δ of BNKLT-*x*/0.10 and BNKLT-0.22/*y* ceramics. There are two anomalies (T_d and T_m) in the curves. T_d is the temperature at which the phase transition from ferroelectric (rhombohedral) to anti-ferroelectric phase (tetragonal). T_m corresponds to the temperature at which the ε_r reaches its maximum value. It can be observed that on the one hand, ε_r show pronounced dependence on frequency. With increasing the frequency, ε_r for all ceramics decreases. In the BNKLT system, Na^+, K^+, Li^+, Bi^+ are randomly distributed at A-sites, leading to random local electric fields and elastic distortions. As a result, the ferroelectric ordering of the ceramics as a whole is inhibited and unit diploes are divided into superparaelectric clusters. The reorientation of the cluster polarization in the applied electric field is governed by the relaxation time required for the redistribution of the charge carriers (probably Na^+, K^+, Li^+, Bi^+) around the cluster. Accordingly, the cluster polarization is 'frozen' under a high-frequency electric field, whereas the orientation of the cluster polarization under a low-frequency electric field is allowed, leading to a large dielectric constant value [17]. On the other hand, both T_d and T_m exhibit obvious dependence on the

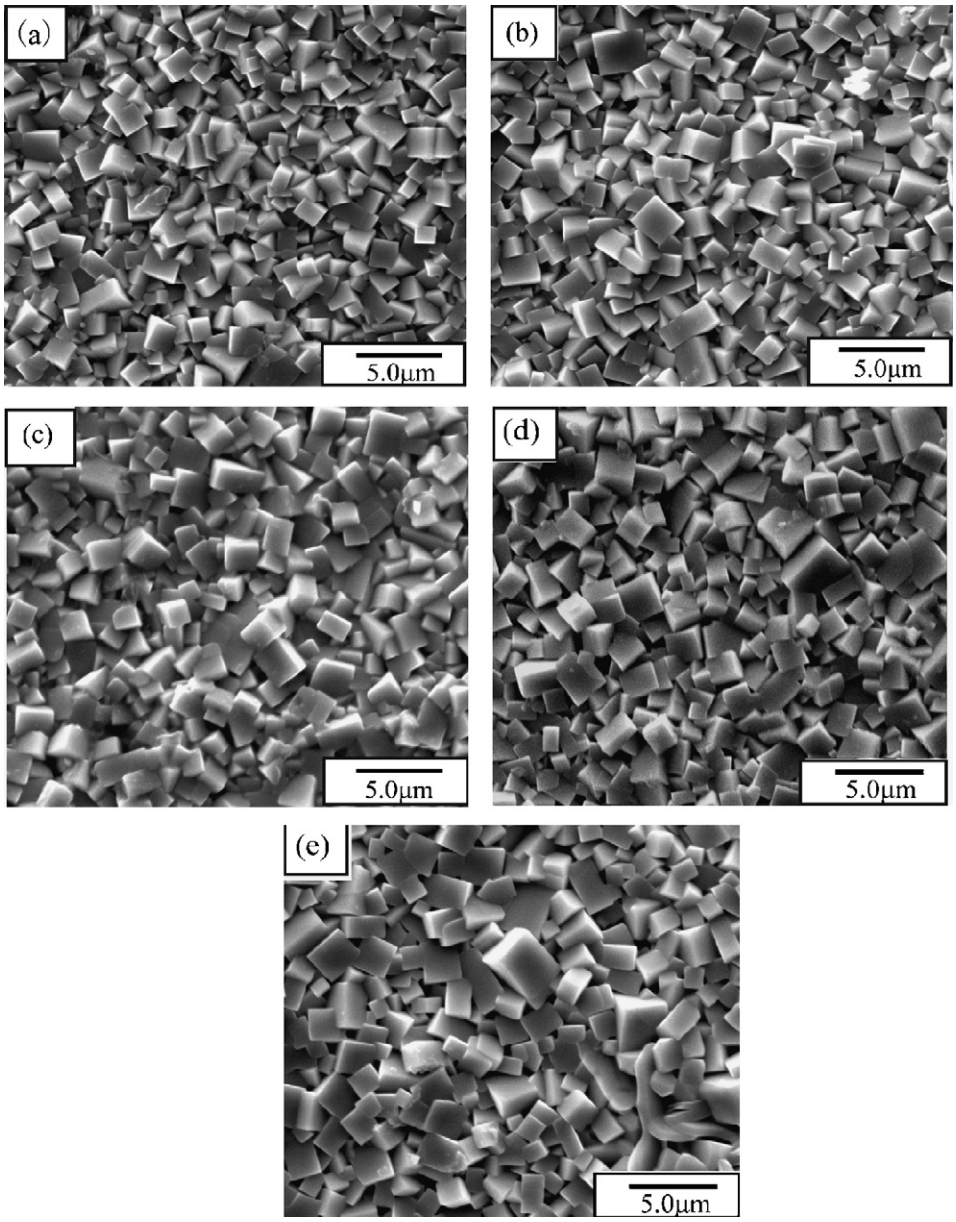

Fig. 4. SEM micrographs of BNKLT-0.22/*y* ceramics: (a) *y* = 0.03; (b) *y* = 0.05; (c) *y* = 0.08; (d) *y* = 0.10; (e) *y* = 0.12.

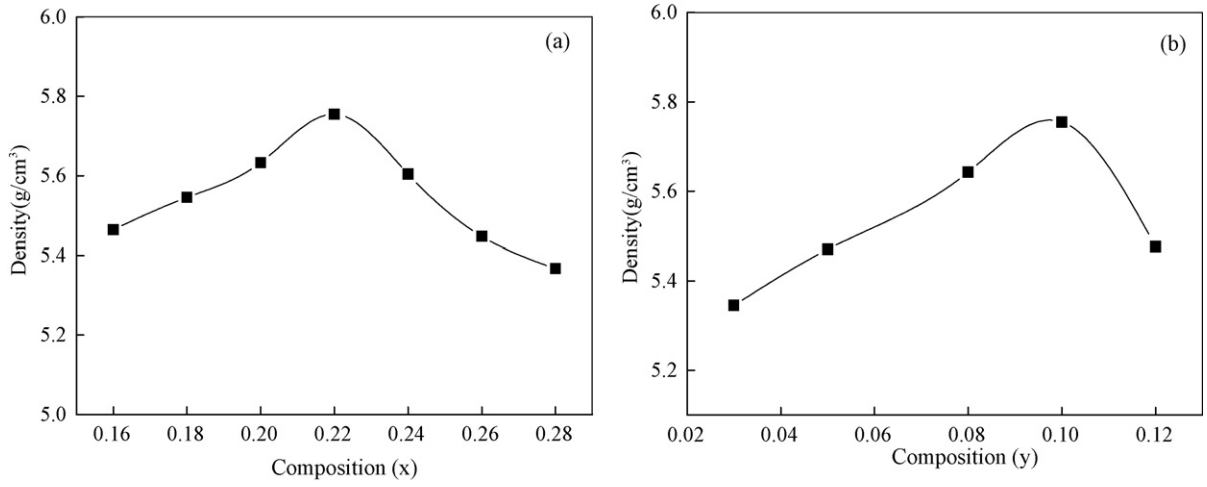

Fig. 5. Density of BNKLT-*x*/*y* ceramics: (a) BNKLT-*x*/0.10; (b) BNKLT-0.22/*y*.

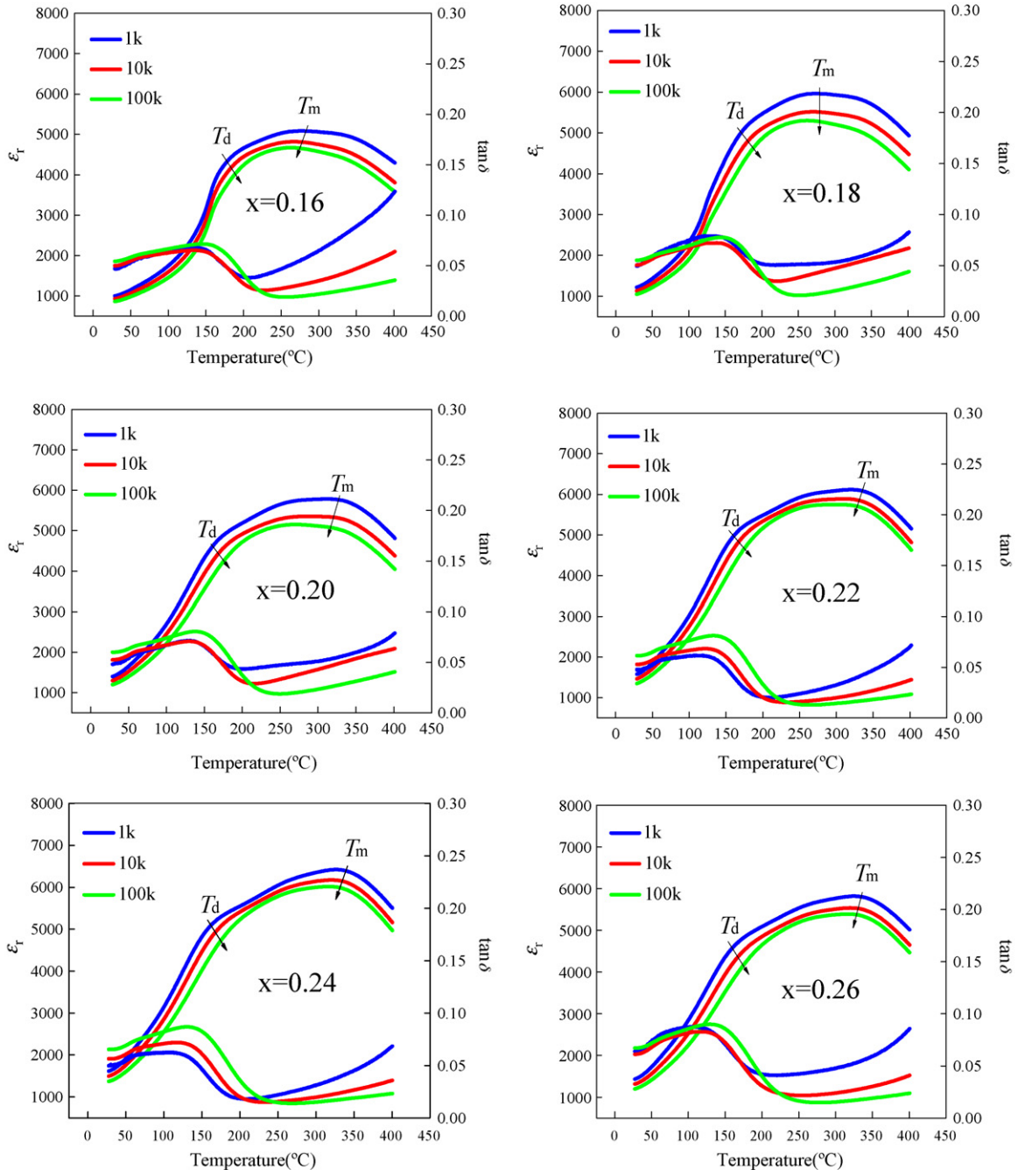

Fig. 6. The temperature dependence of ε_r and tan δ of the BNKLT-x/0.10 ceramics.

frequency. With increasing frequency, T_d moves to lower temperature regions and T_m moves to higher temperature regions. When temperature T is below T_d, ε_r shows strong frequency dependence . The dependence become weaker with T between T_d and T_m, and it becomes obvious again above T_m. The broad ε_r peaks and the character of the temperature dependence of ε_r shows typical relaxation characteristic. The relaxation behavior can be concluded by the compositional fluctuation [18]. For the BNKLT-x/y ceramics, Na^+, K^+, Li^+, Bi^+ ions are randomly distributed at A-site, the coexistence of Na^+, K^+, Li^+ and Bi^+ disordering at A-site may result in the relaxation behavior.

A similar temperature dependence behavior of dielectric loss is also shown in Figs. 6 and 7. tan δ reaches the maximum value around T_d, which is caused by the improvement of the domain wall during the phase transition from ferroelectrics to anti-ferroelectrics. But there is no second dielectric loss peaks occurring. The reason may be that above T_m, tan δ increases sharply, which results from the high conductivity of the ceramics at high temperature.

The dielectric behavior of complex ferroelectrics with diffuse phase transition can be explained by the modified Curie–Weiss law $\varepsilon_m/\varepsilon = 1 + (T - T_m)^\gamma/(2\Delta^2)$ [19–21], where ε_m is the maximum value of the dielectric constant. T_m is the temperature at which ε reaches the maximum γ ($1 < \gamma < 2$) is a constant which is used to express the diffuseness degree of the phase transition. When $\gamma = 1$, the materials with this type of phase transition belong to normal ferroelectrics; when $1 < \gamma < 2$, the materials belongs to relaxor ferroelectrics; when $\gamma = 2$, the materials belongs to ideal relaxor ferroelectrics. Fig. 8 shows $\ln[(\varepsilon_m - \varepsilon)/\varepsilon]$ as a function of $\ln(T - T_m)$ for BNKLT $- x$/0.10 and BNKLT $- 0.22/y$ ceramics at 1 kHz. It can be observed that a linear relationship is obtained by linear fitting the experimental

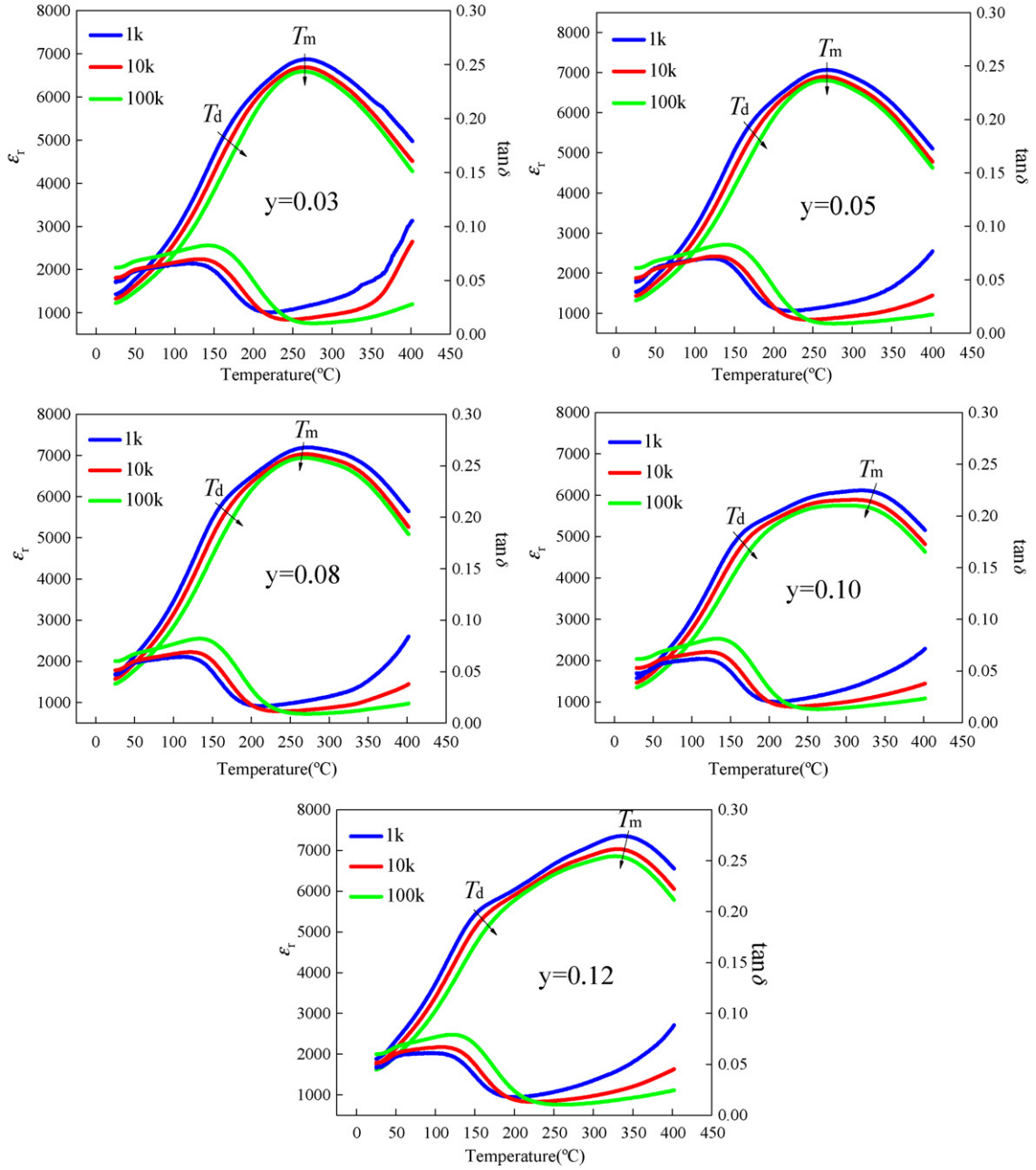

Fig. 7. The temperature dependence of ε_r and tan δ of the BNKLT-0.22/y ceramics.

data. The diffuseness exponent γ of all ceramics is between 1 and 2, which means the phase transition of all ceramics shows the diffuse characteristic. This is in accordance with results of Figs. 6 and 7.

Fig. 9 shows T_d and T_m as a function of x for BNKLT-x/0.10 and y for BNKLT-0.22/y ceramics. It can be seen for BNKLT-x/0.10 and BNKLT-0.22/y ceramics, either increasing x or increasing y has little effect on T_d, which means the crystalline structure does not transform. And all ceramics have of rhombohedral symmetry structure. It agrees with the results of Figs. 1 and 2. In addition, either increasing x or y can increase T_m, which favors the application of BNT-based ceramics.

Fig. 10 shows the P–E hysteresis loops of BNKLT-x/y ceramics. It can be seen that BNKLT-x/0.10 ceramics with x = 0.18 is not well saturated. As x increases, the loops become relatively saturated and almost rectangular due to the decrease of E_c in Fig. 10(a). It can also be seen that P_r increases with increasing x. Besides, well saturated loops can be observed in BNKLT-0.22/y ceramics [Fig. 10(b)]. With increasing y to 0.10, P_r reaches the maximum value (31.92 μC/cm^2). Both P_r and E_c show the similar variation. But the variation of E_c is not as distinct as that of P_r As y increases from 0.05 to 0.10, E_c increases from 30.46 to 32.40 kV/cm slightly. The optimum ferroelectric properties (P_r = 31.92 μC/cm^2, E_c = 32.40 kV) of the ceramics are obtained at x = 0.22 and y = 0.10.

Fig. 11 shows the piezoelectric and dielectric properties for BNKLT-x/0.10 ceramics. When x = 0.16, dielectric constant d_{33} and electromechanical factor K_p are 139 pC/N and 0.26, respectively. With increasing x, d_{33} and K_p reach the maximum values of 203 pC/N and 0.31 at x = 0.22. Further increasing x to 0.26, d_{33} and K_p decrease to 166 pC/N and 0.18 [Fig. 11(a)]. It can be seen from Fig. 11(b) that when x = 0.16, ε_r shows the value of 668. With increasing x, the maximum values of ε_r (1118) can be obtained at x = 0.22. As x increases, the variation of tan δ is not obvious. Fig. 12 shows the piezoelectric and dielectric properties for BNKLT-0.22/y ceramics. The variation tendency of d_{33} is similar to that of K_p.

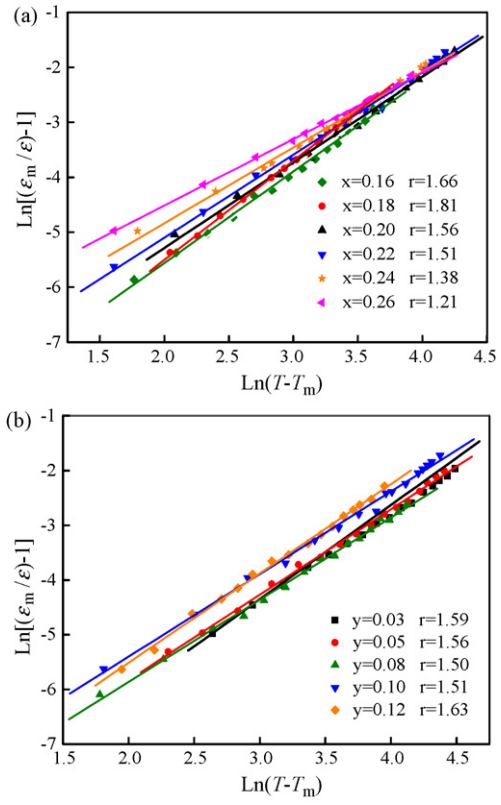

Fig. 8. $\ln[(\varepsilon_m - \varepsilon)/\varepsilon]$ as a function of $\ln(T - T_c)$ for ceramics measured at 1 kHz.

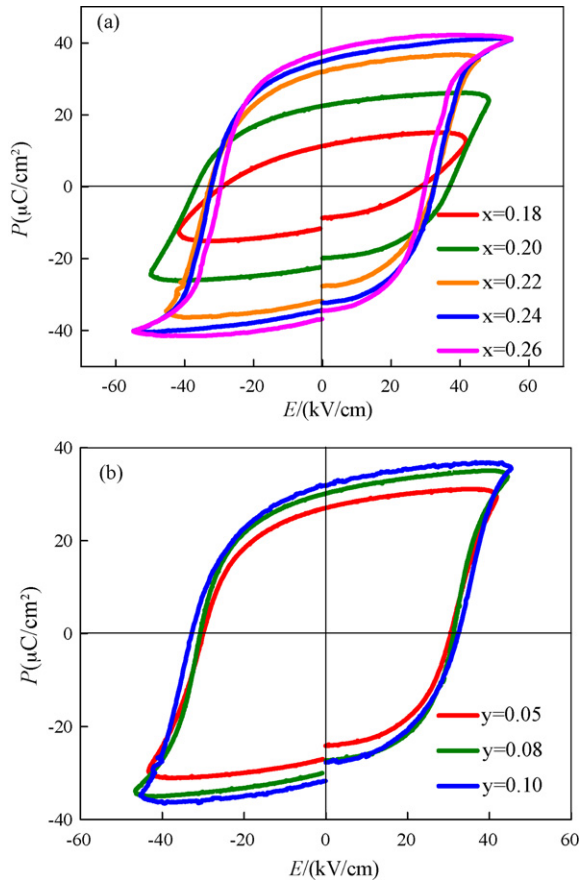

Fig. 10. *P–E* hysteresis loops of BNKLT-*x*/*y* ceramics: (a) BNKLT-*x*/0.10; (b) BNKLT-0.22/*y*.

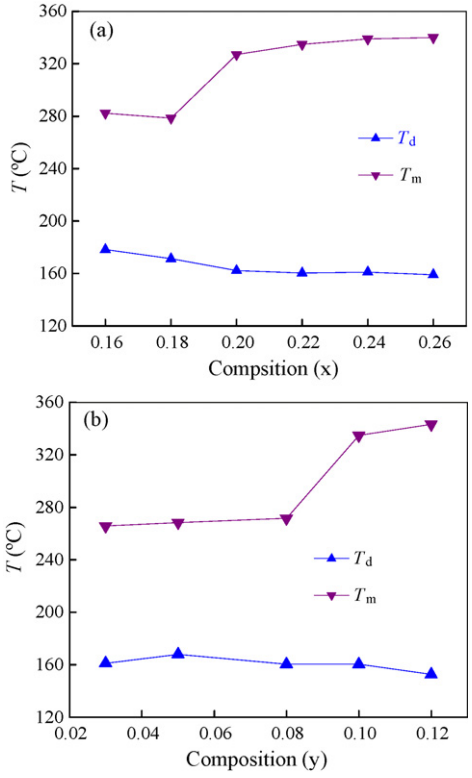

Fig. 9. Variations of T_d and T_m for the ceramics with different *x* and *y*.

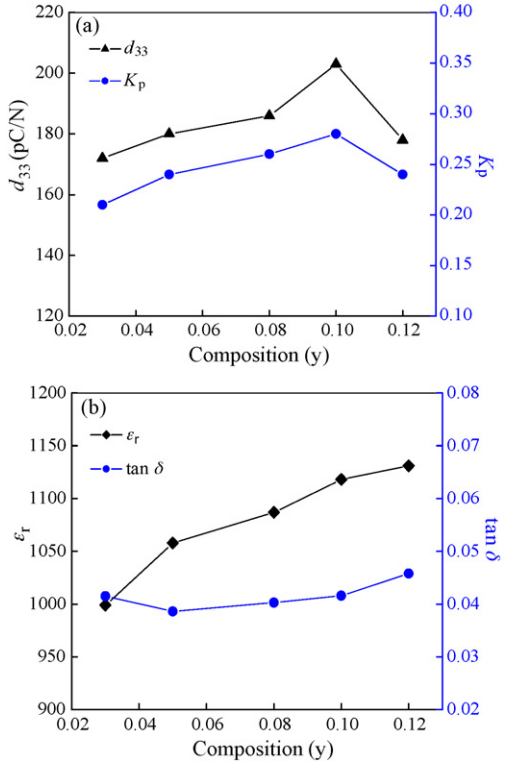

Fig. 11. Piezoelectric (a) and dielectric (b) properties for BNKLT-*x*/0.10 ceramics.

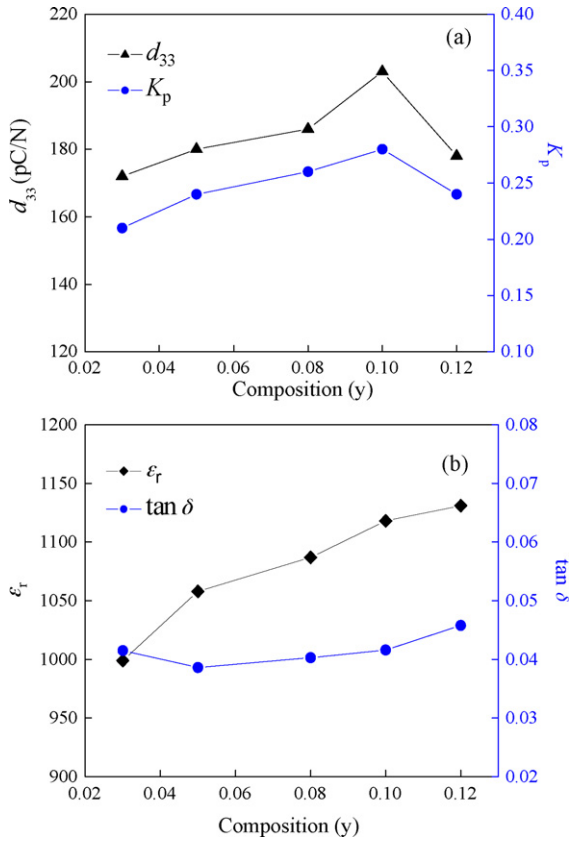

Fig. 12. Piezoelectric (a) and dielectric (b) properties of BNKLT-0.22/y ceramics.

The relative low values (172 pC/N and 0.21) are located at $y = 0.03$. With increasing y to 0.10, d_{33} and K_p reaches the maximum values of 203 pC/N and 0.31. Further increasing y to 0.12, d_{33} and K_p decrease to 178 pC/N and 0.24 sharply (Fig. 12(a)). With increasing y, ε_r and tan δ increases (Fig. 12(b)). It can be concluded that the enhanced piezoelectric properties may be attributed to the strong ferroelectricity (low E_c and large P_r) and improvement in the densification. Low E_c makes the ceramics easily poled and large P_r is beneficial to the piezoelectric properties.

4. Conclusions

BNKLT-x/y lead-free piezoelectric ceramics have been prepared. All samples possessed pure perovskite phase, indicating that K^+ and Li^+ have diffused into the lattice. The SEM images indicate with increasing $Bi_{0.5}K_{0.5}TiO_3$ content, the grain size decrease. But with increasing $Bi_{0.5}Li_{0.5}TiO_3$ content, the variation of the grain size is opposite. All ceramics undergo two phase transitions from ferroelectric to anti-ferroelectric and from anti-ferroelectric to paraelectric. The ceramics show relaxor characteristics which is due to disordering of A-site cations. Either increasing x or y can increase T_m, but has little effect on the T_d. Ferroelectric properties are enhanced with increasing x. On the other hand, with increasing y, both P_r and E_c increase. But the variation of E_c is not as distinct as that of P_r. Introducing BKT and BLT into BNT can promote the ferroelectric properties, thus improving the piezoelectric properties. The optimum electrical properties can be obtained at $x = 0.22$ and $y = 0.10$, which are as follows: $P_r = 31.92\ \mu C/cm^2$, $E_c = 32.40$ kV/cm, $\varepsilon_r = 1118$, tan $\delta = 0.041$, $d_{33} = 203$ pC/N and $K_p = 0.31$.

Acknowledgments

This work was supported by National Science Foundation of China (NSFC) (Grant No. 20771070), Natural Science Research Program of Shaanxi Province (Grant No. 2005B16) and Foundation of Doctorial Program in China (No. 20070718004). Thanks for the Innovation Foundation of Shaanxi Normal University for graduate students.

References

[1] G.A. Smolenskii, V.A. Isupov, A.I. Agranovskaya, N.N. Krainik, Sov. Phys. Solid State 2 (1961) 2651.
[2] T. Takenaka, K. Maruyama, K. Sakata, Jpn. J. Appl. Phys. 30 (9B) (1991) 2236.
[3] T. Takenaka, K. Sakata, Ferroelectrics 95 (1989) 153.
[4] H. Nagata, T. Takenaka, Jpn. J. Appl. Phys. 36 (1997) 6055.
[5] C.G. Xu, D.M. Lin, K.W. Kwok, Solid State Sci. (2007), doi:10.1016/j.solidstatesciences.2007.11.003.
[6] Z.P. Yang, B. Liu, L.L. Wei, Y.T. Hou, Mater. Res. Bull 43 (2008) 81–89.
[7] Z.W. Chen, J.Q. Hu, Ceram. Int. (2008), doi:10.1016/j.ceramint.2007.09.110.
[8] G.F. Fan, W.Z. Lu, X.H.W.F. Liang, Appl. Phys. Lett. 91 (2007) 202908.
[9] Alain Brice Kounga, Shan-Tao Zhang, Wook Jo, Torsten Granzow, Jürgen Rödel, Appl. Phys. Lett. 92 (2008) 222902.
[10] D.M. Lin, K.W. Kowk, H.L.M. Chan, Solid State Ionics 178 (2008) 1930–1937.
[11] Y.M. Li, W. Chen, Q. Xu, J. Zhou, Y. Wang, H.J. Sun, Ceram. Int. 33 (2007) 95–99.
[12] C.G. Xu, D.M. Lin, K.W. Kwok, Solid State Sci. 10 (2008) 934–940.
[13] P. Kantha, K. Pengpat, P. Jarupoom, U. Intatha, G. Rujijanagul, T. Tunkasiri, Curr. Appl. Phys. 9 (2009) 460–466.
[14] M.K. Zhu, L.Y. Liu, Y.D. Hou, H. Wang, H. Yan, J. Am. Ceram. Soc. 90 (1) (2007) 120–124.
[15] X.P. Jiang, L.Z. Li, M. Zeng, H.L.W. Chan, Mater. Lett. 60 (2006) 1786–1790.
[16] Y.W. Liao, D.Q. Xiao, D.M. Lin, J.G. Zhu, P. Yu, L. Wu, X.P. Wang, Ceram. Int. 33 (8) (2007) 1445–1448.
[17] C.S. Tu, I.G. Siny, V.H. Schmid, Phys. Rev. B 49 (1994) 11550.
[18] N. Setter, L.E. Cross, J. Appl. Phys. 51 (8) (1980) 4356–4360.
[19] I.A. Santos, J.A. Eiras, J. Phys. Condens. Matter 13 (50) (2001) 11733–11740.
[20] A.E. Glazounov, A.K. Taganstev, A.J. Bell, Phys. Rev. B 53 (17) (1996) 11281–11284.
[21] X.P. Jiang, L.Z. Li, M. Zeng, H.L.M. Chan, Mater. Lett. 60 (15) (2006) 1786–1790.